

Bacteria–protist interactions and organic matter degradation under P-limited conditions: Analysis of an enclosure experiment using a simple model

T. F. Thingstad

Department of Microbiology, University of Bergen, Jahnebakken 5, N-5020 Bergen, Norway

H. Havskum

The International Agency for ¹⁴C-determination, VKI, Agern Allé 11, DK-2970 Hørsholm, Denmark

H. Kaas, T. G. Nielsen, and B. Riemann

Department of Marine Ecology and Microbiology, National Environmental Research Institute, Fredriksborvej 399, DK-4000 Roskilde, Denmark

D. Lefevre and P. J. le B. Williams

School of Ocean Sciences, University of Wales, Bangor, U.K.

Abstract

An enclosure experiment was performed in the brackish layer of a Norwegian fjord, a system where both phytoplankton and bacterial growth have previously been hypothesized to be phosphorus (p) limited. All enclosures had a succession pattern characterized by an initial autotrophic phase with positive net community production, increasing phytoplankton primary production, and chlorophyll, followed by a heterotrophic phase with decline in primary production, negative net community production, increased community respiration, bacterial production, and biomass. Daily additions of phosphate increased the amplitudes of both the autotrophic and the heterotrophic phases of this succession. Because no stimulating effect of glycine addition on bacterial production or on community respiration was observed, the delay in bacterial response could not easily be explained as a delay in production or availability of carbon substrates for the bacteria. An alternative hypothesis is that bacterial production is regulated by a combination of P-limited bacterial growth rate and predatory control of bacterial biomass. A simple numerical model based on this hypothesis was able to reproduce the main features of the observed pattern of succession.

Consumption rate of organic material by bacteria can be expressed as $Y_{BC}^{-1}\mu_B B$, where Y_{BC} is the bacterial growth yield, μ_B is the specific bacterial growth rate, and B is the bacterial biomass or abundance (depending on the units used for Y_{BC}). A full understanding of the dynamic control of bacterial consumption of organic carbon in the natural environment thus requires an understanding of how all three of these multiplicative factors are controlled by physiological properties of bacteria and by the interactions between the bacteria and the rest of the pelagic ecosystem (Thingstad and Lignell 1997). A correct model for these controlling factors is not only interesting in the limited perspective of understanding bacterial production per se. There is an increasing body of evidence suggesting that degradable dissolved organic car-

bon (DOC) may accumulate in the photic zone during the productive season (Copin-Montégut and Avril 1993; Carlson et al. 1994; Williams 1995). Because the combined trophic control of bacterial biomass and growth rate may limit the ability of bacteria to degrade the labile DOC produced in the system, this model offers a theoretical mechanism for DOC accumulation in addition to the hypothesis that accumulation is a result of direct production of recalcitrant material by processes in the food web (Thingstad et al. 1997). The importance of understanding these mechanisms is highlighted by suggestions of DOC transport to the deep being as important as the vertical flux of particles in transporting organic carbon out of the photic zone and therefore out of contact with the atmosphere (Legendre and Gosselin 1989; Copin-Montégut and Avril 1993; Murray et al. 1994; Thingstad and Rassoulzadegan 1995; Williams 1995).

Several relationships involving Y_{BC} , μ_B , and B have to be integrated in models aiming for a complete description of bacterial consumption of DOC. These models include aspects such as bacterial growth yield under different types of limitation (Pirt 1982; Thingstad 1987), type of substrate limiting bacterial growth rate in the natural environment (Elser et al. 1995), the kinetic aspects of lability of the organic material (Billen 1990; Keil and Kirchman 1994; Lindell et al. 1995), algal–bacterial competition for mineral nutrients (Yull Rhee 1972; Bratbak and Thingstad 1985; Wheeler and Kirchman 1986), and predatory control of bacterial biomass

Acknowledgments

We thank W. Martinsen and E. F. Skjoldal for skillful technical assistance and Anita Jakobsen and the crew of RV *Håkon Mosby* for assistance in carrying out the enclosure experiment. The idea of using a hybrid steady state description of the microbial part of the food web emerged during one of many fruitful discussions with J. Baretta, VKI, Denmark, on how to model the planktonic ecosystem. We also thank an anonymous reviewer for suggesting to incorporate also the full differential equation description.

This work was done as part of the EU MAST-II program, contract MAS2-CT92-0031-‘MEICE’, with additional support from the Norwegian Research Council and MAST contract MAS3-CT97-0016 ‘MEDEA.’

and abundance (Fenchel 1982). Although many discussions of bacterial growth in natural environments explicitly or implicitly assume that bacterial growth is carbon limited (e.g., Bratbak and Thingstad 1985; Billen and Servais 1990), there is no a priori reason to believe that this must always be the case. Recent experiments with additions of mineral and organic substrates to untreated or filtered water samples from the photic zone have shown that phosphorus (p) may be the primary limiting factor for bacterial growth in marine environments such as the Mediterranean (Zweifel et al. 1993; Thingstad et al. 1998), the Gulf of Mexico (Pomeroy et al. 1995), and the Sargasso Sea (Cotner et al. 1997). In coastal areas influenced by freshwater, P limitation of the heterotrophic bacteria was suggested by Zweifel et al. (1995) to retard degradation of DOC in the Baltic. In the brackish layer of the Sandsfjord fjord system in western Norway, a pronounced luxury consumption of added orthophosphate in the 0.2–1- μm size fraction lead Thingstad et al. (1993) to suggest P limitation of bacterial growth rates.

A previously suggested simple model, based on the trophic interactions of algal–bacterial competition for mineral nutrients and protozoan predation on bacteria (the BAFP system, Fig. 1 shaded box), summarizes the essential aspects of consumption of labile organic matter by bacteria with a mineral nutrient-limited growth rate (Thingstad et al. 1997). An adaptation of this type of model to an enclosure experiment is given here. Some of the important theoretical properties of a community of this type have been confirmed experimentally in chemostat systems (Pengerud et al. 1987), including dependence of steady state algal–bacterial coexistence upon the presence of a predator selective for the bacteria. The model also includes a reduction in the degradation of organic matter (glucose) when both predators (protozoa) and competitors (algae) are added to a bacterial culture, as opposed to an increase in degradation following the addition of bacterial predators only.

Because the expected responses of this system to allochthonously added orthophosphate and easily degradable DOC are very different and depends upon whether bacterial growth rate is C or P limited, we conducted enclosure experiments with each of these treatments alone and in combination, expecting this to allow us to reject at least one of the two alternative hypotheses of carbon and mineral nutrient-limited growth of heterotrophic bacteria.

Materials and Methods

Study site, enclosure construction, and sampling—The investigations were carried out in the brackish layer of Hylsfjord (59°30'N, 6°30'E) which is an arm of the Sandsfjord fjord system on the southwestern coast of Norway. The microbial phosphorus metabolism and its relation to the hydrography of this fjord system has been described previously (Thingstad et al. 1993).

Eight enclosures made of polyethylene (90% light transmission), 1 m in diameter and 2 m in depth (approximate initial volume = 1.6 m³), were tied to individual floating frames and placed along the inside an octagonal floating pontoon of approximately 10 m diameter. This design gave

a U-shaped alignment of the enclosures, with the opening of the U facing southwest as the arrangement giving a reasonable compromise between the two requirements of minimizing wind stress and shading. To avoid biased results due to potential unequal shading, enclosures were placed in the clockwise sequence (K1, P3, C5, CP7, K2, P4, C6, CP8), where 1 and 2, 3 and 4, etc., were parallels with identical additions; K = controls, P = orthophosphate, C = glycine (carbon), and CP = orthophosphate + glycine, respectively (Table 1). Nutrients were added each day at 2000 h according to the scheme in Table 1. Phosphate and nitrate were added from sterile aqueous solutions of 100 mM KH₂PO₄ and 1,000 mM NaNO₃, respectively. Glycine was added as preweighed amounts dissolved in water from the individual enclosures immediately prior to addition. All enclosures, including controls, received nitrate with the intention of preventing the complication of shifting the systems into N limitation.

The enclosures were filled between 900 and 1200 h on 5 July 1995 using a centrifugal pump with an all-plastic pump head and tubing. The pump was fixed at one position at 1 m depth through the whole filling procedure. The hose was moved between enclosures so that each enclosure was filled in portions of approximately 0.1 m³ to approximate a parallel filling of the enclosures minimizing any effects of potential fluctuation in water quality at the pump intake. The water column in each enclosure was kept continuously mixed throughout the experiment using an airlift system consisting of a 2-m plastic tube suspended vertically in the enclosures with compressed air injected into the tubes at 1 m depth (Egge and Heimdal 1994). The salinity in the enclosures was 7 psu. Temperatures increased slightly during the experimental period from 12.5°C to 14.2°C.

Water samples were collected using a 3-liter plastic water sampler and were pooled in 10-liter polyethylene carboys, one for each enclosure. The carboys were marked to ensure consistent use for samples from one enclosure and were rinsed with water from the corresponding enclosure prior to filling. Water was collected between 800 and 900 h and immediately brought to the RV *Håkon Mosby* positioned close (minutes) to the enclosures.

Oxygen flux—Dissolved oxygen concentrations were determined by Winkler titrations using a PC-based system with a photometric end point detector (Williams and Jenkinson 1982). Borosilicate glass bottles (50 ml, four replicates) were used to perform light- and dark-bottle incubations for 24 ± 0.5 h in all eight enclosures. For all incubations, the oxygen concentration was measured at the start and end of the incubation.

Phytoplankton and bacteria—Pigments were extracted for 24 h in ethanol from duplicate filters (Jespersen and Christoffersen 1987). Total absorbance at 665 nm was measured spectrophotometrically, and a specific absorption coefficient of 83.4 liters g⁻¹ cm⁻¹ was applied (Wintermans and De Mots 1965).

¹⁴C-determined primary production was measured in situ in 50-ml bottles with 12 μCi NaH¹⁴CO₃ (International Agency for ¹⁴C Determination). Samples were incubated for a

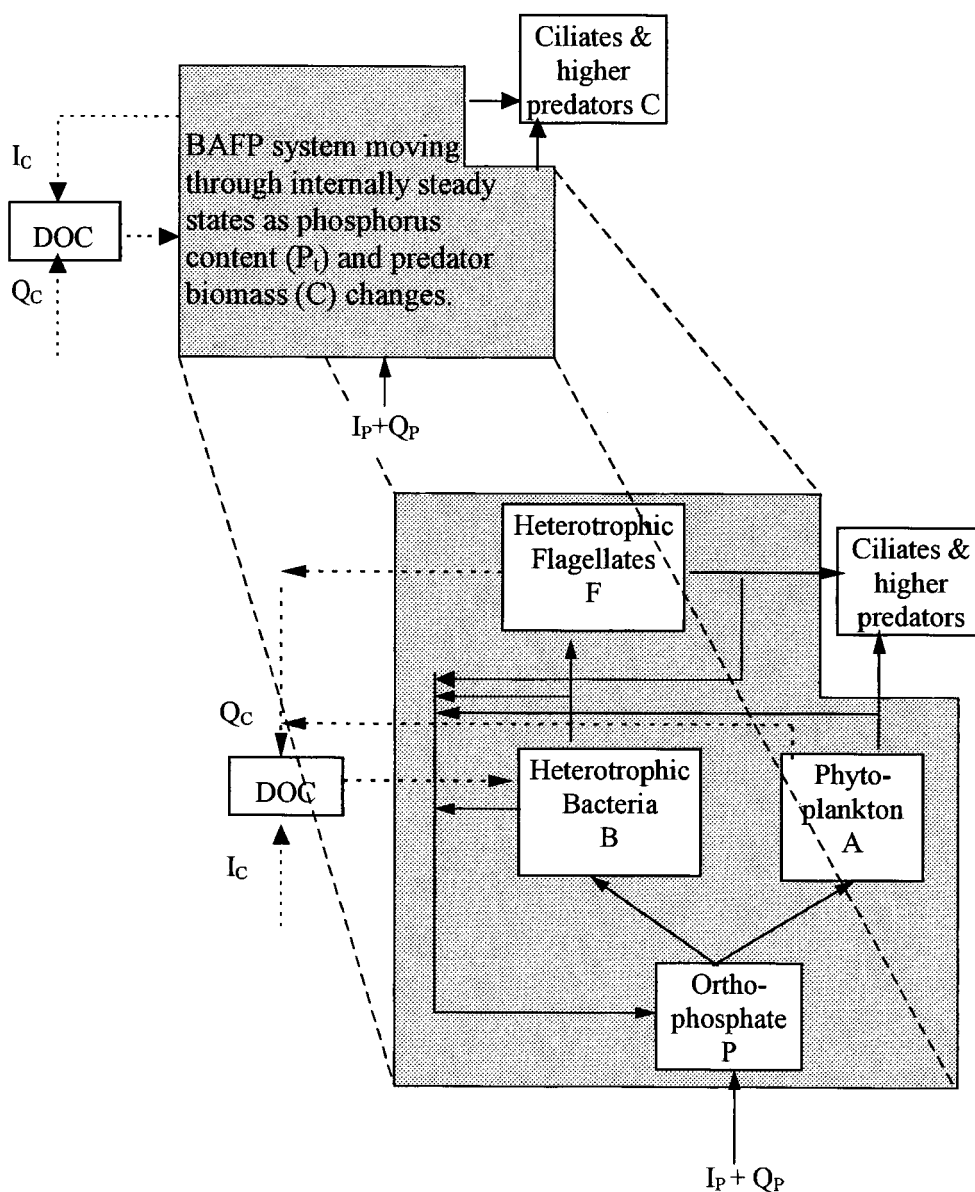


Fig. 1. Model used for analyzing the results of the enclosure experiments. The model consists of the inner BAFP system (within the shaded area), to which phosphorus is added allochthonously (I_p) and autochthonously (Q_p , phosphate originating from the system in the enclosures but from outside the BAFP system) as orthophosphate and from which phosphorus is removed by external predators (C). The BAFP system is assumed to have a sufficiently rapid internal dynamics to always be in internal equilibrium according to the (changing) amount of P in the inner system (P_i) and external grazing pressure. Details of the BAFP system are shown in blown-up view. Solid arrows denote P flows. Dotted lines denoting production and consumption of DOC are added for clarification but are immaterial for the state within the BAFP system as long as bacterial growth rate is P limited. DOC is dissolved organic carbon, and I_c is the external input of carbon.

Table 1. Daily additions (mmol m^{-3}) to the enclosures.

Type of addition	Enclosure	PO_4 (P)	Glycine (C)	NO_3
Control	K1, K2	0	0	2
PO_4	P3, P4	0.1	0	2
Glycine	C5, C6	0	4	2
PO_4 + glycine	CP7, CP8	0.1	4	2

half-day (noon to sunset) at 0.5 m and 1.5 m depths in their respective enclosures. Immediately after incubation, 10-ml volumes were filtered through 0.45- μm Sartorius membranes 25 mm in diameter. The filters were treated with fuming HCl for 5 min and placed in glass vials with 10 ml Ecoscint (BN Plastic), and the radioactivity was assayed in a scintillation counter (Rack-Beta, LKB, Vallac) after storage of at least 24 h in the dark. Duplicate samples were taken from each of

the mesocosms and from the open fjord. The average production per cubic meter per day was calculated from the areal production computed from the depth distribution of the two samples. No measurements of extracellular losses of carbon were made.

Bacteria were enumerated using 4',6-diamidino-2-phenylindole (DAPI, Porter and Feig 1980). Cells were classified as $<2 \mu\text{m}$ and $>2 \mu\text{m}$. The $>2\text{-}\mu\text{m}$ fraction was dominated by filamentous bacteria $\leq 200 \mu\text{m}$ long. They were similar in length to the spines of *Chaetoceros wighamii* but were clearly discernible from these spines because *Chaetoceros* spines have a characteristic curvature, stained less with DAPI, and are wider than the bacteria. ^3H -thymidine incorporation was carried out according to Fuhrman and Azam (1980; slightly modified by van Looij and Riemann 1993). A conversion factor of 1.1×10^{18} cells mol^{-1} thymidine incorporated was applied (Riemann et al. 1987), and bacterial cell volumes were measured according to Lee and Fuhrman (1987). ^{14}C -leucine incorporation into protein was measured according to Simon and Azam (1989) with addition of 50 nM ^{14}C -leucine. Isotope dilution was measured according to Riemann and Azam (1992). Triplicate samples and blanks were incubated with additions of ^{14}C -leucine ranging from 1 to 100 nM. On the basis of the hyperbolic incorporation kinetics, a calculation of the maximum leucine incorporation rate was obtained using nonlinear regression. The isotope dilution approach was carried out nine times (twice in each of the four manipulated enclosures and once in the open fjord); the average ($\pm\text{SD}$) dilution factor was 1.7 ± 0.3 ($n = 9$). The average value was used for all the rate measurements.

Nutrients—Soluble reactive phosphorus (SRP) was determined in triplicate samples using standard molybdenum blue reagents with subtraction of turbidity measured on each sample (Koroleff 1976). A 5-cm cuvette was used in a microprocessor-controlled spectrophotometer with 4 significant digits in the optical density reading (Shimadzu UV1201), with four readings of each filling of the cuvette, and with one washing and two fillings of the cuvette from each of the three replicates of each sample.

For other nutrients, two 30-ml samples were taken of the filtrate from the chlorophyll filtration and frozen immediately. Within 2 months, concentrations of soluble inorganic nutrients (ammonium, nitrite, nitrate, silicate) were analyzed using an ASA automatic nutrient analyzer (Olsen and Lundgren 1984).

Phosphate uptake—Turnover time for bioavailable orthophosphate and uptake in size fractions of >10 , 1–10, and 0.2–1 μm were measured for 10-ml samples incubated with carrier-free $^{33}\text{PO}_4$ in polyethylene vials using on-deck incubators with running seawater. After an incubation time of 5–15 minutes (adjusted according to expected turnover time), a cold chase of 0.1 mM KH_2PO_4 was added, and the contents were filtered through 10-, 1-, and 0.2- μm polycarbonate filters, avoiding any washing (Suttle et al. 1990). The radioactivity on the filters was measured by scintillation liquid counting, uptake in size fractions was computed by subtraction, and turnover time T was calculated from the formula

$T = -t/\ln[(R_f - R_b)/R_t]$, where R_f , R_b , and R_t are the radioactivities of the filter, the filter of a blank fixed with ca. 50 μl formalin, and the total radioactivity added to the sample, respectively. Particulate P in the same size fractions was determined for samples collected by serial filtration onto 47-mm polycarbonate filters following the procedure described by Thingstad et al. (1993).

Microzooplankton—For identification and enumeration of ciliates and heterotrophic dinoflagellates, two 100-ml samples were used. One was fixed with 2% Lugol solution, and the other was fixed with 1% glutaraldehyde. The samples were kept cold and dark until examination. The ciliates were identified to species or morphotype according to Montagne and Lynn (1991). The heterotrophic dinoflagellates were identified according to Dodge (1985). Unidentified specimens were placed in size classes.

Depending on the concentration of protozoa, 20-, 50-, or 100-ml samples were allowed to settle for 24 h, and contents were counted using the Utermöhl technique (Nikon Diaphot 200 inverted microscope with epifluorescence). Biomass was calculated from biovolume, which was converted to carbon using 0.11 pg C μm^{-3} for ciliates and athecate dinoflagellates and 0.13 pg C μm^{-3} for thecate dinoflagellates (Edler 1979). The biovolume calculations were based on measurements of linear dimensions using appropriate geometrical shapes.

Results

O_2 production and consumption—After an initial slightly negative net community production (heterotrophic processes dominating), all enclosures went through a cycle with a phase of positive net production (photosynthetic processes dominating) for 3–4 days and then back to negative net community production (Fig. 2). The two periods are referred to here as the autotrophic and heterotrophic phases, respectively. The oxygen balance was not affected by the glycine additions, neither in enclosures where it was added alone (C5 and C6 as compared with K1 and K2) nor when it was added together with phosphate (CP7 and CP8 as compared with P3 and P4; Fig 2). However, addition of phosphate increased the length of the autotrophic phase and the amplitude of both the autotrophic and the consecutive heterotrophic phase (P3 and P4 as compared with K1 and K2, and CP7 and CP8 as compared with C5 and C6). Community respiration increased in all enclosures throughout the experimental period, most rapidly in enclosures with phosphate added from 7 July (Fig. 2). Gross productivity culminated around 7 July in enclosures without added phosphate (K and C enclosures) and around 9 July in enclosures with phosphate added (P and CP enclosures).

Chlorophyll and ^{14}C -determined primary production—The autotrophic phase corresponded to a period of increasing chlorophyll (Chl) concentrations (Fig. 3). The major difference between enclosures was an increased growth rate in all enclosures receiving phosphate. Minimum growth rates (Table 2) computed from fitting exponential curves to net increase in chlorophyll corresponded to generation times of

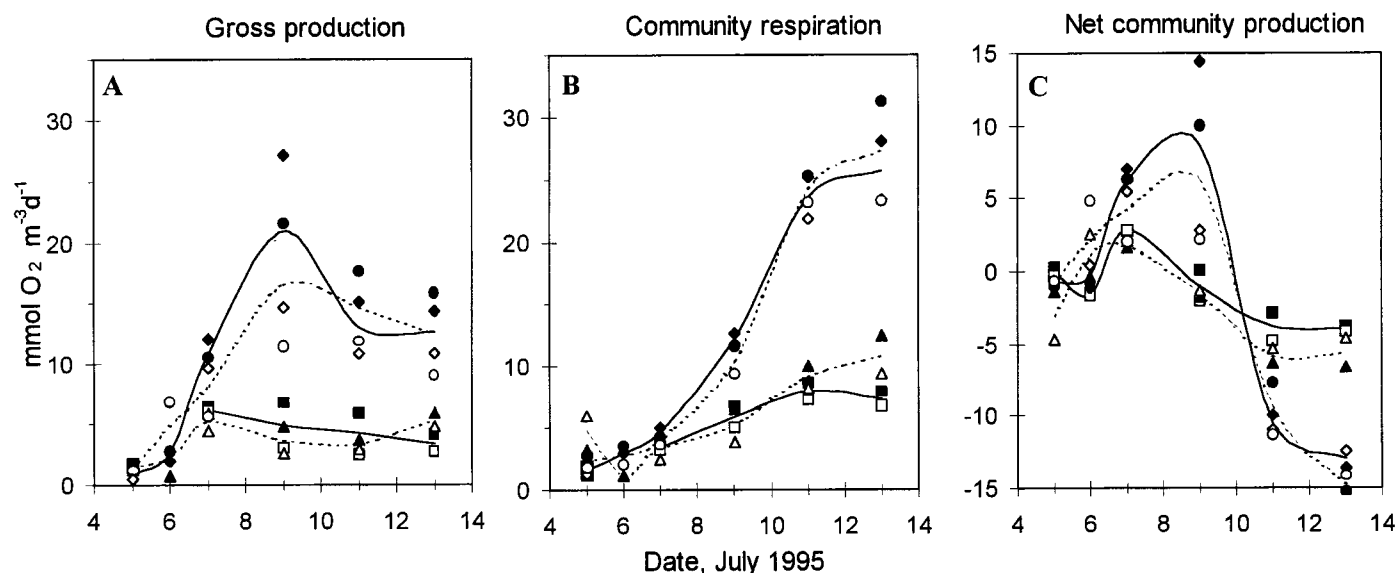


Fig. 2. Gross production (A), community respiration (B), and net community production (C) in K (squares), P (diamonds), C (triangles), and CP (circles) enclosures. Solid and open symbols of same type represent parallel enclosures. Means for the two K enclosures and for the two P enclosures are indicated by smoothed solid lines, and means for the two C and the two CP enclosures are indicated with smoothed dotted lines.

1.2 and 1.3 days for the P and CP enclosures, respectively, as compared with 2.1 and 2.3 days in the K and C enclosures, respectively. As a result, much higher chlorophyll concentrations were reached in enclosures receiving phosphate (ca. 20 mg Chl m^{-3} in P and CP enclosures, respectively, compared with ca. 7 mg Chl m^{-3} in K and C enclosures, respectively). No effect on growth rates could be seen from the glycine additions (Table 2), but chlorophyll levels in the semistationary phase after 8 July were slightly but consistently higher in enclosures receiving glycine (Fig. 3), with a mean of 25% higher values in the C than in the K enclosures and a mean of 16% higher values in CP than in P enclosures for the period 9–13 July.

In the fjord outside the enclosures, chlorophyll levels fluctuated initially and then levelled off at a value lower than that inside the enclosures (Fig. 3).

Primary production as estimated by the ^{14}C technique, and oxygen changes were affected similarly. There was no effect of glycine, but there was a marked effect of phosphate (Fig. 3). Productivity index (primary production/Chl *a*) increased as a response to phosphate addition (Table 2), suggesting an increase in phytoplankton growth rate in P and CP enclosures. Mean (\pm SD) apparent photosynthetic quotient (mol O_2 produced per mol C fixed, Table 2) for all measurements was 1.3 ± 0.3 . This value is similar to the value of 1.26 ± 0.6 reported by Daneri et al. (1994).

Bacterial abundance and bacterial production by 3H -thymidine and ^{14}C -leucine—A major response in total bacterial numbers was only found in the heterotrophic phase after 9 July in enclosures receiving phosphate (Fig. 4). Initially, the bacterial community contained a significant portion ($\approx 10^5$ ml) of large ($>2 \mu m$) filamentous bacteria (Fig. 4). The abundance of these large bacteria generally increased throughout the experiment in all enclosures. At the end of

the experiment they accounted for about 60% of a bacterial C-biomass of 35–40 and 15–20 mmol C m^{-3} in enclosures with and without P added, respectively (Havskum and Hansen 1997).

Bacterial production estimated from thymidine incorporation (Fig. 4) increased in two steps, one approximate doubling through the first day after filling of the enclosures and then a major second increase in the heterotrophic phase. The second increase was about twice as large in enclosures receiving phosphate, with a final mean (\pm SD) value of 0.13 ± 0.01 mol C $m^{-3}d^{-1}$ in P and CP enclosures as compared with 0.07 ± 0.01 mol C $m^{-3}d^{-1}$ in K and C enclosures. The leucine method gave production estimates of similar magnitude and pattern, but with consistently lower estimates in enclosures receiving glycine and a decrease in activity at the end of the experimental period, not observed with thymidine (Fig. 4). Using the thymidine-based values and the community respiration, the mean (\pm SD) respiration ratio was 1.2 ± 0.6 mol O_2 consumed by the community per mol C produced as bacterial biomass, with a statistically insignificant tendency towards higher quotients in enclosures receiving orthophosphate (1.0 ± 0.3 , 1.3 ± 0.5 , 1.1 ± 0.9 , and 1.3 ± 0.6 in K, P, C, and CP enclosures, respectively). This value is much lower than the 4.3 found in a previous study using similar techniques (recalculated from the ratio of net: gross bacterial production of 0.16 found by Daneri et al. 1994) and implied a bacterial growth yield of 45%.

Inorganic nutrients, orthophosphate uptake, and particulate P—SRP concentrations in the enclosures were in the range 0.02–0.1 mmol m^{-3} . After some initial fluctuations, values stabilized with a tendency towards slightly higher values in enclosures receiving phosphate (Fig. 5). If the SRP values represent biologically available orthophosphate, high

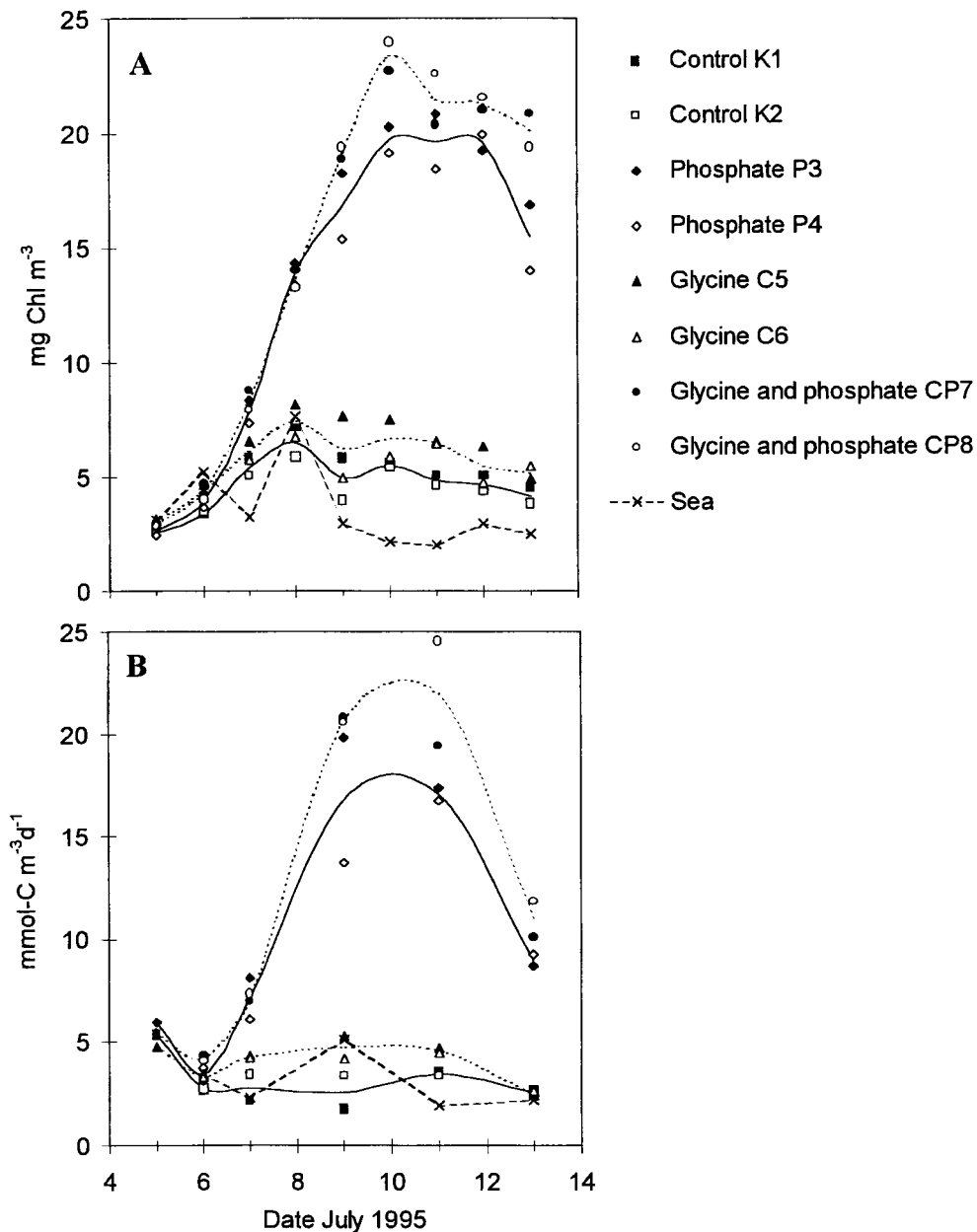


Fig. 3. Chlorophyll *a* concentrations (A) and ^{14}C -determined primary production (B) in control enclosures K (squares), P enclosures receiving phosphate (diamonds), C enclosures receiving glycine (triangles), and CP enclosures receiving glycine and phosphate (circles) and in the sea (crosses) (see Fig. 2).

orthophosphate uptake rates are obtained as illustrated by calculations for 11 July (Table 3).

In enclosures without phosphate added, nitrate + nitrite concentrations increased linearly during 7–12 July, with a slope of $1.65 \pm 0.04 \text{ mmol m}^{-3} \text{ d}^{-1}$ ($R^2 = 0.998$), indicating a fixed consumption rate of $\approx 0.35 \text{ mmol m}^{-3} \text{ d}^{-1}$ of the $2 \text{ mmol NO}_3 \text{ m}^{-3} \text{ d}^{-1}$ added. In enclosures with P added, nitrate concentrations dropped to close to the detection level during 9–11 July (Fig. 5). Nitrite concentrations remained low ($\leq 0.17 \text{ mmol m}^{-3}$) in all enclosures.

Following an initial decrease in silicate in all enclosures

for the first 2–3 days, rapid silicate consumption continued in enclosures with phosphate added, resulting in silicate depletion in P and CP enclosures from 9 July to the end of the investigation (Fig. 5).

In all enclosures, as in the open sea the turnover time for bioavailable orthophosphate remained relatively short ($< 2 \text{ h}$, Fig. 6). In enclosures without P addition (K1, C5), the turnover time decreased continuously from the beginning of the experiment until a minimum of about 6 min was reached on 11 July. In enclosures receiving phosphate (P3, CP7), the turnover time remained at the original level until 8 July,

Table 2. Chlorophyll-based net phytoplankton growth rate in the autotrophic phase of the experiment, productivity indexes based on ^{14}C primary production, and photosynthetic quotient based gross productivity from O_2 measurements and ^{14}C primary production.

Enclosures	Growth rate* \dagger (d^{-1})	Productivity index \dagger ($\text{mgC mgChl}^{-1} \text{d}^{-1}$)	Photosynthetic quotient \ddagger ($\text{mol O}_2 \text{ mol C}^{-1}$)
Controls: K1, K2	0.33 ± 0.04	7.6 ± 0.7	1.7 ± 0.2
Phosphate added: P3, P4	0.57 ± 0.04	10.1 ± 0.8	1.2 ± 0.2
Glycine added: C5, C6	0.30 ± 0.03	8.2 ± 0.6	1.1 ± 0.3
Glycine and phosphate added: CP7, CP8	0.52 ± 0.02	10.7 ± 1.1	1.0 ± 0.1

* R^2 ranged from 0.975 to 0.992.

\dagger Period 5–9 July ($n = 4$).

\ddagger Period 6–13 July ($n = 5$) in P, C, and CP enclosures, 7–13 July ($n = 4$) in K enclosures.

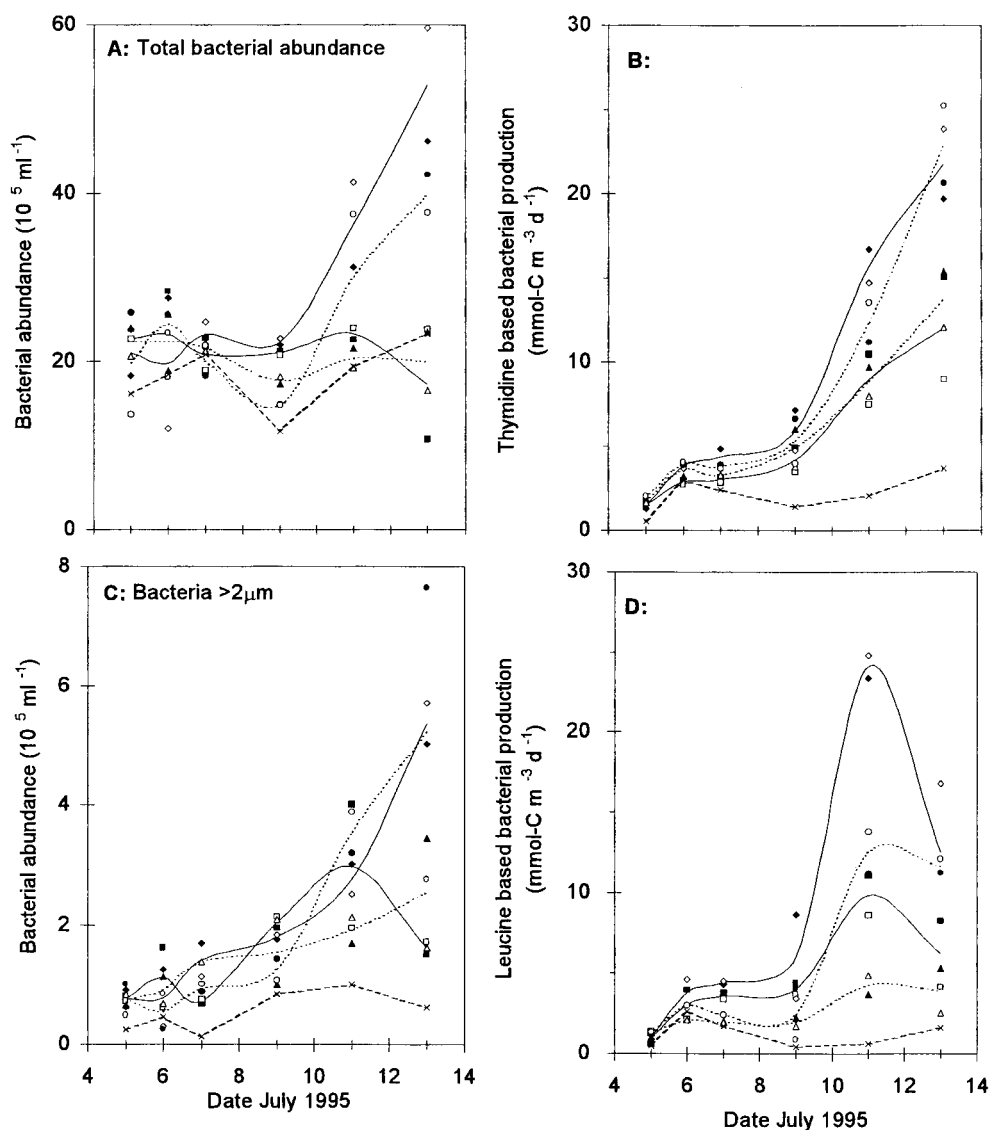


Fig. 4. Total bacterial abundance (A) and abundance of large ($>2 \mu\text{m}$) bacteria (C) in enclosures and in the open sea. Bacterial production estimates are from incorporation of thymidine (B) and leucine (D) (see Fig. 2).

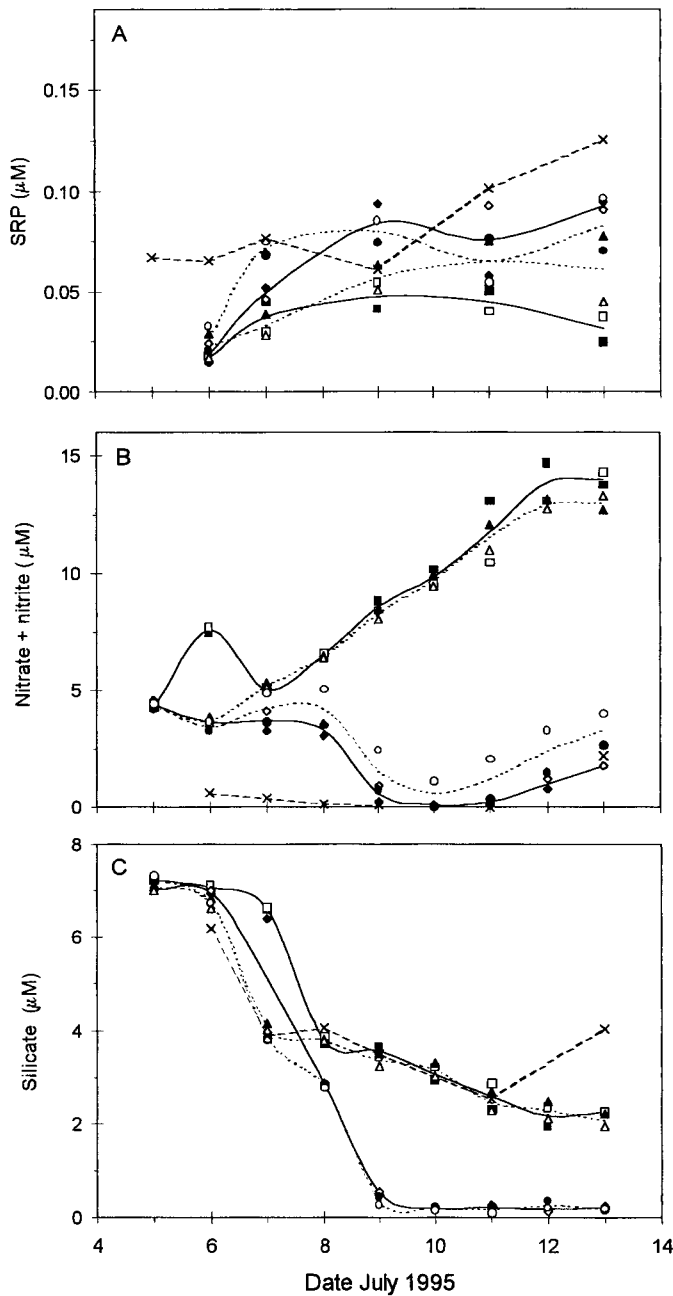


Fig. 5. Concentrations of soluble reactive phosphorus (A), nitrate + nitrite (B), and silicate (C) (see Fig. 2).

followed by a decrease also in these enclosures to reach the same minimum of ca. 6 min on 11 July.

At the beginning of the experiment (5 July), relative mean (\pm SD) orthophosphate uptake by the size fractions >10 , 1–10, and 0.2–1 μm was $40\% \pm 3\%$, $32\% \pm 4\%$, and $26\% \pm 2\%$, respectively, of total uptake (for enclosures C1, P3, C5, and CP7). At the end of the experiment (13 July), the contribution by the three size fractions was $23\% \pm 3\%$, $40\% \pm 7\%$, and $37\% \pm 5\%$, respectively. In all enclosures, there was thus a tendency towards decreasing relative uptake by the largest size fraction, a pattern opposite to that observed in the fjord where the $>10\text{-}\mu\text{m}$ size fraction increased its

Table 3. Mean of chemically determined orthophosphate concentrations (SRP) in the mesocosms 7–13 July ($n = 4$) and in the sea 5–13 July ($n = 6$). Corresponding uptake estimates for 11 July based on dividing the SRP value by the orthophosphate turnover time obtained from $^{33}\text{PO}_4$ uptake.

Enclosures	SRP (mmol m^{-3}) mean	SE	Phosphate uptake rate ($\text{mmol m}^{-3} \text{h}^{-1}$)
Controls			
K1	0.040	0.005	0.41
K2	0.041	0.005	ND
Phosphate added			
P3	0.075	0.011	0.50
P4	0.076	0.011	ND
Glycine added			
C5	0.064	0.009	0.71
C6	0.045	0.006	ND
Glycine and phosphate added			
CP7	0.072	0.002	0.77
CP8	0.078	0.009	ND
Sea	0.086	0.012	0.09

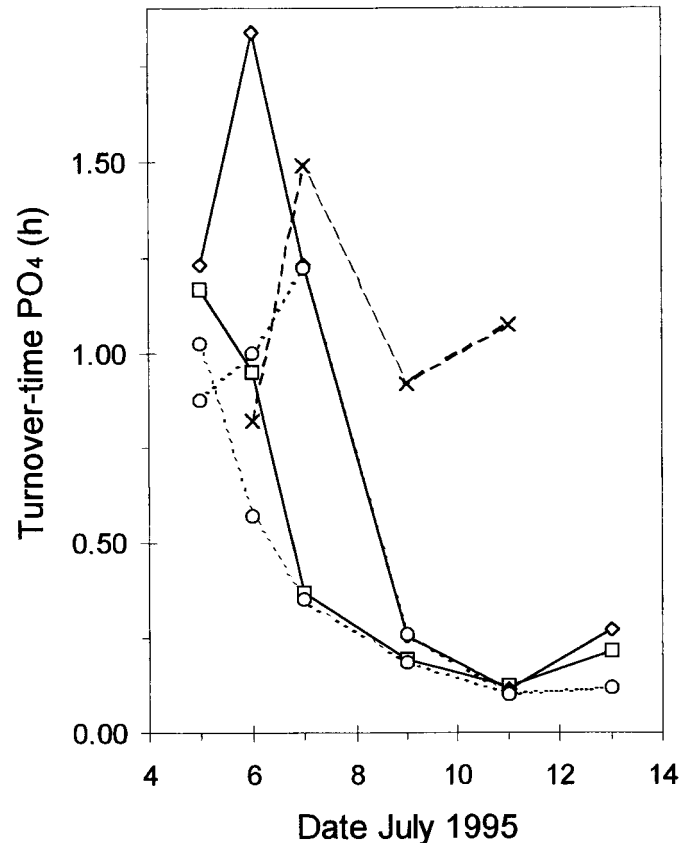


Fig. 6. Turnovertime for orthophosphate in enclosures K1, (\square), P3 (\diamond), C5 (\triangle), and CP7 (\circ) and in the sea (\times). Solid lines between points are used for enclosures without glycine additions, dotted lines are for enclosures with glycine, and a broken line for the open sea.

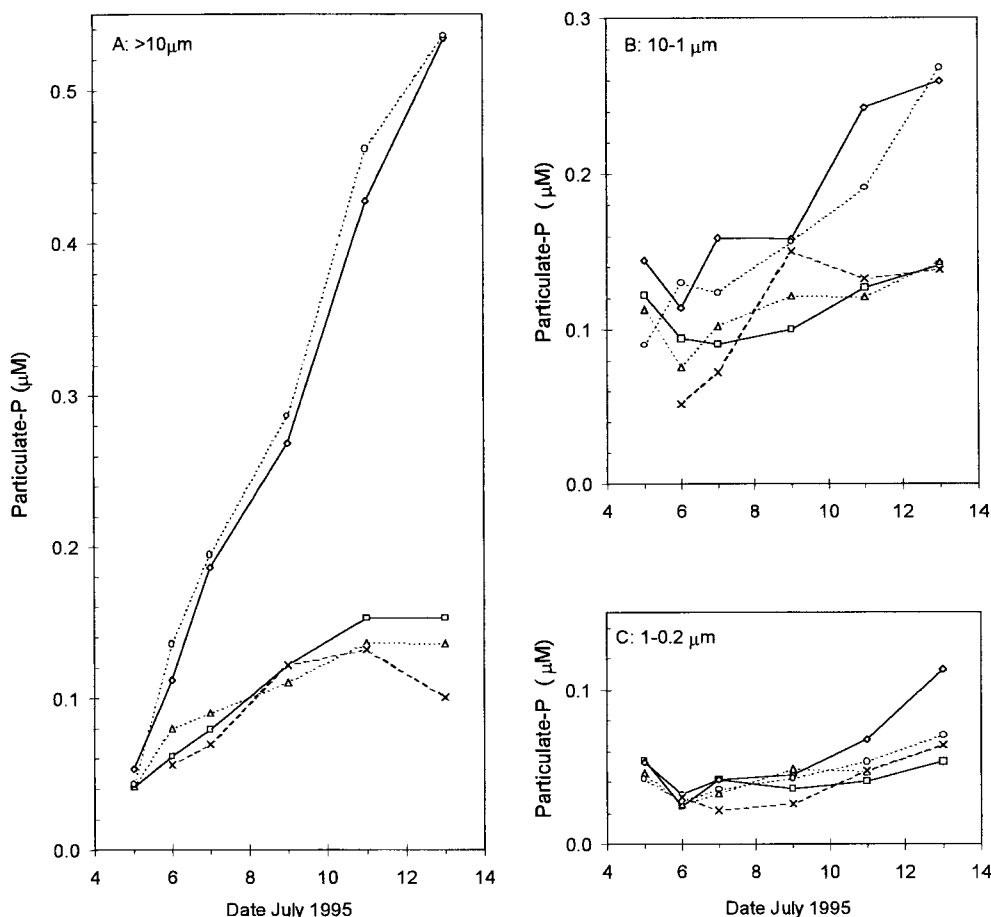


Fig. 7. Particulate P in size fractions of (A) >10 , (B) $1-10$, and (C) $0.2-1 \mu\text{m}$ in enclosures K1, (\square), P3 (\diamond), C5 (\triangle), and CP7 (\circ) and in the sea (\times).

share of orthophosphate uptake through the experimental period. Only minor differences in uptake were observed among enclosures (data not shown).

The main fraction of the P added was transferred into the $>10\text{-}\mu\text{m}$ particulate size fraction (Fig. 7). At the end of the experiment, the $>10\text{-}\mu\text{m}$ fraction in P3 and CP5 contained $0.53 \text{ mmol P m}^{-3}$, an increase of $0.49 \text{ mmol P m}^{-3}$ since the beginning of the experiment. Of the 0.80 mmol m^{-3} P added, 61% was thus transferred to the $>10\text{-}\mu\text{m}$ fraction. Because this fraction only amounted to 20–40% of orthophosphate uptake, there must have been a significant transfer of P from smaller to larger organisms, presumably via predation.

Micrograzers—Starting from initial biomasses of 0.13 and $0.14 \text{ mmol C m}^{-3}$ in enclosures K1 and P3, respectively, near-exponential growth in ciliate biomass was observed (Fig. 8) in P3, with a maximum generation time of $1.8 \pm 0.1 \text{ d}$ (5–13 July, $R^2 = 0.993$, $n = 5$), as estimated from the net increase in biomass. In K1, growth in ciliate biomass culminated after about 1 week. Fitting of exponential growth to the period 5–9 July gave a maximum generation time of $1.6 \pm 0.1 \text{ d}$ ($R^2 = 0.999$, $n = 3$). In addition, there was a fairly large population of heterotrophic dinoflagellates (Fig. 8), with an initial biomass of 0.47 and $0.48 \text{ mmol C m}^{-3}$ in K1 and P3, respectively. Within the experimental period, this

subpopulation did not show any consistent pattern of change (Fig. 8). In this experiment, grazing on phytoplankton by mixotrophic dinoflagellates was also observed (Havskum and Hansen 1997).

Description of model

Analytical solutions allow nontrivial relationships to be derived, and cause–effect relationships in the model therefore are more easily understood than when analysis is based purely on numerical solutions. Unfortunately, analytical solutions for our BAFP system (Fig. 1) can only be derived under several simplifying assumptions. We have chosen here to explore in particular the usefulness of the simplifying assumption that dynamics within the BAFP system are sufficiently fast for the distribution of phosphorus within the BAFP system to approach internal steady state in the time interval from nutrient addition to the time of measurement. This internal steady state is a function of the amount of phosphorus contained in the BAFP system (P_i) and the amount of ciliates (C). These two variables change dynamically governed by coupled differential equations. This type of hybrid model therefore produces a sequence of steady states for the BAFP system as an approximation to the pattern of succession that would be produced by a more tradi-

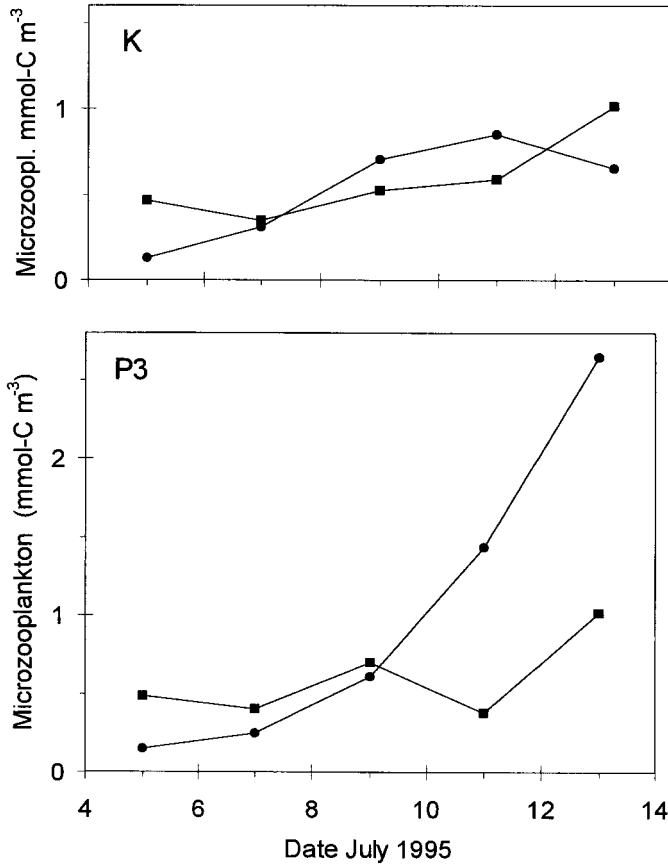


Fig. 8. Biomass of ciliates (●) and heterotrophic dinoflagellates (■) in enclosures K1 and P3.

tional description using differential equations for all variables. The suggested advantage of this hybrid technique is an improvement in our ability to understand the mechanisms regulating the behavior of the system (Tables 4, 5).

Although phytoplankton growth rate is assumed always to be limited by phosphate, the system will work in two qualitatively different ways, depending upon whether bacterial growth rate is assumed to be P or C limited.

The simplest case is when C limitation is assumed. With C-limited bacterial growth rate, an external input (I_C) of organic C would be consumed by bacteria without any competition for this substrate, and a rapid increase should be observable in bacterial production. At steady state in the DOC pool, one would have

$$B_{\text{prod.}} = Y_{BC} (Q_C + I_C), \quad (13)$$

where I_C and Q_C are the allochthonous input and autochthonous (originating from the system in the enclosures) production rates, respectively, of degradable organic carbon. Assuming autochthonous production Q_C to be on the order of 50% of primary production, an allochthonous input I_C equal to the primary production should increase bacterial production by a factor of 3. One would also expect this I_C to increase the bacterial share of phosphate uptake and in general induce a shift from a phytoplankton-based to a bacteria-based food web. Such a shift towards a bacteria-based

Table 4. Equations describing the steady state of phosphorus distribution inside the BAFP system of Fig. 1.

The steady state assumption (growth = sum of losses) gives the following set of conditions:

Phytoplankton ($dA/dt = 0$):

$$\alpha_{AP}PA = \delta_A A. \quad (1)$$

Bacterial predators ($dF/dt = 0$):

$$Y_{FB}\alpha_{FB}BF = \delta_F F. \quad (2)$$

Bacteria ($dB/dt = 0$) (when mineral nutrient limited):

$$\alpha_{BP}PB = \alpha_{FB}BF + \delta_B B. \quad (3)$$

In addition, there is the mass balance requirement that the sum of the different pools equals the system nutrient content P_t :

$$P_t = P + A + B + F. \quad (4)$$

The solution to this set of equations (provided all variables > 0) is (Thingstad et al. 1997)

$$P^* = \frac{\delta_A}{\alpha_{AP}} \quad (5)$$

$$B^* = \frac{\delta_F}{Y_{FB}\alpha_{FB}} \quad (6)$$

$$F^* = \alpha_{FB}^{-1} \left(\frac{\alpha_{BP}}{\alpha_{AP}} \delta_A - \delta_B \right) \quad (7)$$

$$A^* = P_t - (P^* + B^* + F^*). \quad (8)$$

Note how only phytoplankton concentration A^* is dependent upon phosphorus content P_t of the subsystem, whereas concentration of bacteria, B^* , and bacterial growth rate, $\mu_B = \alpha_{BP}P^*$, are proportional to the loss rates δ_F and δ_A of heterotrophic flagellates and phytoplankton, respectively. Assuming the two specific loss rates δ_A and δ_F to be given by $\delta_A = \alpha_{CA}C$ and $\delta_F = \alpha_{CF}C$, where α_{CA} and α_{CF} are ciliate clearance rates for phytoplankton and heterotrophic flagellates, respectively; bacterial production B_{prod} will be given by:

$$B_{\text{prod}} = \mu_B B = \alpha_{BP}P^*B^* = Y_{FB}^{-1} \frac{\alpha_{BP}}{\alpha_{AP}\alpha_{FB}} \delta_A \delta_F = Y_{FB}^{-1} \frac{\alpha_{BP}\alpha_{CA}\alpha_{CF}}{\alpha_{AP}\alpha_{FB}} C^2. \quad (9)$$

Hence, bacterial biomass and production will increase proportionally to C , and C^2 , respectively, as phosphorus is transferred from the BAFP system to ciliates.

Ciliate biomass, C , is computed from the differential equation

$$\frac{dC}{dt} = Y_{CA}\delta_A A^* + Y_{CF}\delta_F F^*. \quad (10)$$

Total phosphorus in the system, P_T , is computed from

$$\frac{dP_T}{dt} = Q_P + I_P, \quad (11)$$

and total phosphorus inside the BAFP system, P_t , is from the balance

$$P_t = P_T - C. \quad (12)$$

food web has been described in enclosures receiving glucose (Parsons et al. 1981).

When bacterial growth rate is assumed to be P limited, the internal steady state is a function of the phosphorus con-

Table 5. Symbols and values used in the mathematical model.

Symbols used	Meaning	Initial value
P_T	Total phosphorus in all compartments	0.220 mmol m ⁻³
P_i	Total phosphorus inside the BAFP system = ($P_T - C$) =	0.200 mmol m ⁻³
P	Orthophosphate P (from Eq. 5)	0.001 mmol m ⁻³
B	Bacterial biomass P (from Eq. 6)	0.029 mmol m ⁻³
F	Bacterivorous flagellates biomass P (from Eq. 7)	0.013 mmol m ⁻³
A	Phytoplankton biomass P (from Eq. 8)	0.157 mmol m ⁻³
C	Ciliate biomass P	0.020 mmol m ⁻³
* Steady state values of B, A, F, and P		
Constants		
α_{BP}	Bacterial affinity for orthophosphate	5.00 m ³ mmol ⁻¹ h ⁻¹
α_{AP}	Phytoplankton affinity for orthophosphate	4.00 m ³ mmol ⁻¹ h ⁻¹
α_{FB}	Flagellate clearance rate for bacteria	0.40 m ³ mmol ⁻¹ h ⁻¹
α_{CA}	Ciliate clearance rate for phytoplankton	0.20 m ³ mmol ⁻¹ h ⁻¹
α_{CF}	Ciliate clearance rate for flagellates	0.20 m ³ mmol ⁻¹ h ⁻¹
Y_{FB}	Flagellate yield on bacteria	0.34 (dimensionless)
Y_{CA}	Ciliate yield on phytoplankton	0.17 (dimensionless)
Y_{CF}	Ciliate yield on flagellates	0.17 (dimensionless)
δ_B	Bacteria-specific death rate	0.00 h ⁻¹
δ_F	Flagellate-specific death rate	Computed from $\alpha_{CF}C$ h ⁻¹
δ_A	Phytoplankton-specific death rate	Computed from $\alpha_{CA}C$ h ⁻¹
μ_B	Bacteria-specific growth rate	Computed from $\alpha_{BP}P$ h ⁻¹
I_P	Allochthonous input of phosphate	0.100 mmol m ⁻³ d ⁻¹
Q_P	Autochthonous input of phosphate	
	5–8 July	0.030 mmol m ⁻³ d ⁻¹
	8–13 July	0.000 mmol m ⁻³ d ⁻¹

ment (P_i) of the BAFP system and the external grazing pressure (Table 4). The BAFP system will then move through a sequence of steady states as phosphorus is either added to or removed from the BAFP system and as grazing pressure increases with increasing biomass of external predators (C). In these steady states, bacterial growth rate is a function of the concentration of free phosphate, which again is a function of the competition from phytoplankton. If phytoplankton are subject to a high predation pressure, the equilibrium condition for phytoplankton (Eq. 1, Table 4) implies that they have to grow fast, and the equilibrium concentration of free phosphate limiting the growth rate must be high. High predation pressure on phytoplankton thus gives a high bacterial growth rate. If there is a high predation rate on the bacterivorous flagellates, the equilibrium condition for the bacterial predators (Eq. 2, Table 4) requires a high flagellate growth rate and therefore a high food concentration, i.e., a high bacterial biomass. Adding phosphate will increase the internal total P content (P_i) of the BAFP system, but bacterial biomass and growth rate will only be affected as the added phosphate is transferred up the food chain into the ciliate population. The size of the DOC pool is immaterial to the internal state of the BAFP system as long as the concentration is high enough to keep bacterial growth rate P limited. DOC concentration will change according to the differential equation

$$\frac{d}{dt}\text{DOC} = Q_C + I_C - Y_{BC}^{-1}B_{\text{prod}}, \quad (14)$$

where Y_{BC} is the bacterial yield on the carbon source and B_{prod} is bacterial production as given in Eq. 9 (Table 4).

To illustrate how such a model can qualitatively describe the most important aspects of the enclosure experiment, we made the following assumptions:

1. The internal dynamics of the BAFP system are rapid enough to accommodate input and loss rates of the magnitude used here, so that offsets from steady state can be neglected for the 0.5–1 d⁻¹ sampling frequency used here. Between sampling times, however, the system moves from one steady state to another.
2. The specific loss rates δ_F and δ_A of bacterivorous flagellates and phytoplankton are given as the products $\alpha_{CF}C$ and $\alpha_{CA}C$, respectively, where C is the phosphorus content of larger predators (hereafter called ciliates for convenience) and α_{CF} and α_{CA} are the ciliate clearance rates for heterotrophic flagellates and phytoplankton, respectively.
3. Loss of phosphorus from the BAFP system only occurs by the transfer of phosphorus into ciliate biomass.
4. All uptake and predation rates can be written as the product of an affinity constant (clearance rate), the nutrient (food) concentration, and the consumer biomass. For example, bacterial uptake rate for orthophosphate is given as $\alpha_{BP}PB$, and flagellate predation on bacteria is given by $\alpha_{FB}BF$.
5. There are two inputs of orthophosphate to the BAFP system: (1) in all enclosures there is a constant autochtho-

nous input rate Q_p of $0.02 \text{ mmol P m}^{-3} \text{ d}^{-1}$ from 5 to 8 July and (2) in P and CP enclosures there is the additional experimental allochthonous input I_p of $0.10 \text{ mmol P m}^{-3} \text{ d}^{-1}$ for the entire experimental period. The autochthonous source Q_p is assumed to come from the ecosystem enclosed in the mesocosms but originating from outside the BAFP system. The inclusion of this source was necessary to describe the sequence of events in the K and C enclosures and may be hypothesized to be an effect of phosphate released from higher organisms outside the BAFP system. Some such release may have been enhanced by a detrimental effect on larger organisms from either the confinement itself or the filling procedure (centrifugal pump) used for setting up the enclosures.

6. Growth rate of the bacteria is P limited.

With these assumptions and the parameter and initial values given in Table 5, our equations can be solved using a simple spreadsheet calculation. P content of ciliate biomass (C) was calculated using a simple Euler algorithm: for each 1-h time step, ciliate biomass was increased by the amount eaten multiplied by ciliate yield ($Y_{CF}\alpha_{FC}F + Y_{CA}\alpha_{AC}A$) C . The change in phosphorus content (P_i) inside the BAFP system could then be computed as the difference between the input ($Q_p + I_p$) and the predatory loss. Knowing P_i and C , the internal state of the BAFP system could then be computed from the equations in Table 4. The sequence of biomass P in the different compartments, the primary and bacterial productions (assuming molar C:P ratios of 106 and 50 in phytoplankton and bacteria, respectively), and the oxygen balance (assuming a photosynthetic quotient and a respiratory quotient of 1) computed from this algorithm are shown in Fig. 9.

Discussion

High bacterial growth following peaks in phytoplankton abundance can be explained by various models assuming C limitation of bacterial growth rates. These models include a need for hydrolysis of polymeric substrates by bacteria using extracellular enzymes (Billen 1991), excretion of organic compounds by phytoplankton only as they go into nutrient limitation (e.g., Williams 1990), or organic substrates for bacterial growth being released as a function of predatory processes related to the decrease in phytoplankton abundance (Jumars et al. 1989). We found no effect of glycine on community respiration or on thymidine uptake, which would be expected for C limitation of bacterial growth rate. The glycine addition rate of $4 \text{ mmol C m}^{-3} \text{ d}^{-1}$ is of the same magnitude as the ^{14}C -based primary production estimates in enclosures not receiving phosphate (K and C enclosures), and a bacterial use of the glycine as a carbon source should presumably have led to major differences between these enclosures. The minor effects observed from glycine addition are opposite to those expected if bacterial production were stimulated by glycine. Therefore, bacterial growth rate in the enclosures appears to have been phosphorus rather than carbon limited.

In our model, the phytoplankton compartment follows an equation of the type $A = P_i - k_1C + k_2$, where k_1 and k_2

are constants (Eq. 8), while all other compartments increase linearly with ciliate biomass C . The model thus produces a pattern of succession where the added phosphate first is incorporated into phytoplankton biomass; this provides increased food supply for ciliates, which grow, and the increased ciliate biomass eventually leads to a decreasing phytoplankton biomass and an increase in all the other compartments. Through this mechanism, the model reproduces the autotroph-heterotroph sequence observed in the enclosures through an initial increase in phytoplankton biomass (increases linearly with P_i , Eq. 8) and then an increase in the heterotrophs (B and F increasing linearly with C , Eqs. 6, 7) accompanying the decrease in phytoplankton as phosphorus is transferred to ciliate biomass C . In both model (Fig. 9) and experiment, the effect is much more pronounced in the P and CP enclosures because of the larger and uninterrupted input of allochthonous orthophosphate.

When parameter values are chosen as in the example above, the model gives a turnover time of free phosphate of the correct magnitude (≈ 1 h), decreasing through the experimental period in enclosures receiving phosphate (Fig. 10). The modelled decrease in turnover time is, however, not as extensive as that observed in the enclosure, a discrepancy particularly large for the K and C enclosures. Despite a too long turnover time, the model's concentration of free phosphate ($2\text{--}17 \mu\text{mol m}^{-3}$) was much lower than the measured SRP. We believe, however, that the chemical determination of SRP gives values far above what is biologically available in this P-limited environment. This conclusion is supported by the unrealistically high uptake rates computed from combining SRP values and orthophosphate turnover time (Table 3) and is consistent with conclusions reached in previous investigations in the same area (Thingstad et al. 1993).

The model gives a pronounced shift towards bacterial dominance of orthophosphate uptake in the late heterotrophic phase of the experiment (Fig. 10). Such an effect was only vaguely indicated in an observed increased share of orthophosphate uptake in the $0.2\text{--}1\text{-}\mu\text{m}$ size fraction toward the end of the experimental period (data not shown). The use of this size fraction as an indicator of bacterial activity in this experiment was, however, severely complicated by the presence of filamentous bacteria. If one assumes that filamentous bacteria have a P uptake per biomass unit equal to that of small bacteria, the distribution of 60% of bacterial biomass as filamentous and about 40% of orthophosphate uptake in the $0.2\text{--}1\text{-}\mu\text{m}$ size fraction at the end of the experiment suggests that almost all the P uptake could have been in bacteria, i.e., close to the situation predicted by our model (Fig. 10).

Havskum and Hansen (1997) studied grazing in the same experiment as reported here using fluorescently labeled bacteria (FLB) and algae (FLA) with equivalent spherical diameters of 0.9 and $3.4 \mu\text{m}$, respectively. In general accordance with the model used here, they found that FLB were grazed by colorless flagellates in the size range $5\text{--}10 \mu\text{m}$, i.e., corresponding to our model's flagellate group, and FLA were grazed by organisms in the size range $10\text{--}20 \mu\text{m}$, corresponding to our ciliate group. The $10\text{--}20\text{-}\mu\text{m}$ FLA predators consisted, however, of a mixture of ciliates, heterotrophic flagellates, and mixotrophic dinoflagellates. In our

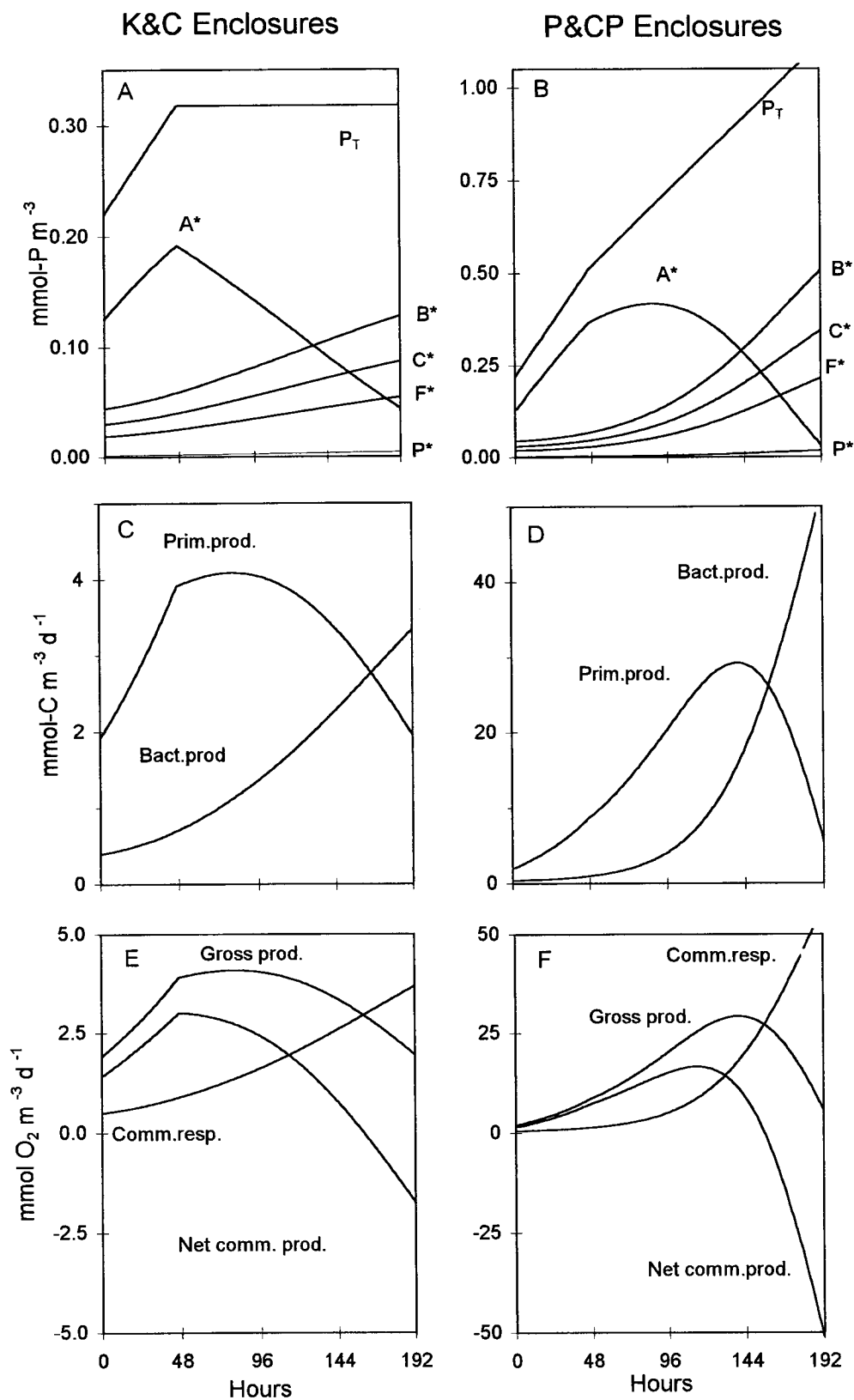


Fig. 9. Model results using parameters and initial values as in Table 5. Panels in left column shows results for K and C enclosures, and panels in right column show results for P and CP enclosures. Note the change in distribution of biomass P (A, B), primary and bacterial production (C, D), and oxygen flux (E, F). Note the difference in scale on the y-axes for the K and C enclosures (left column) and the P and CP enclosures (right column).

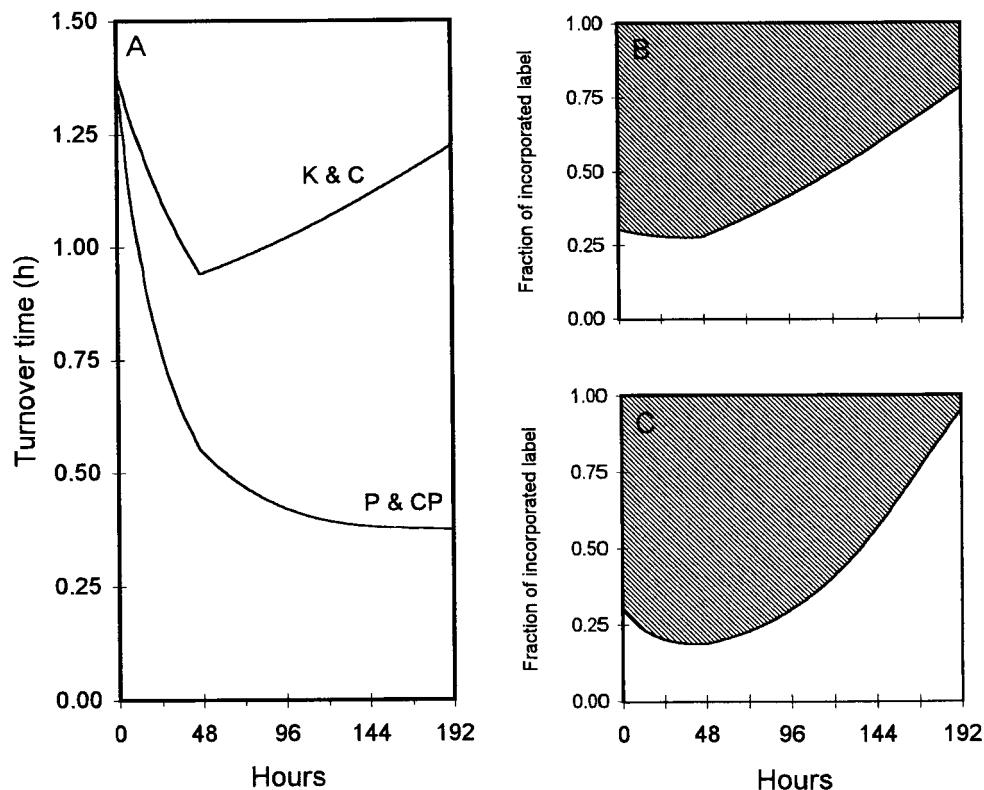


Fig. 10. Model results. Turnover time for orthophosphate (A) and distribution of orthophosphate uptake between bacteria (open area) and phytoplankton (hatched area) in K and C (B) and in P and CP (C) enclosures.

model, the protists are classified as either strict competitors (phytoplankton) or strict predators (heterotrophic flagellates) of bacteria. Mixotrophs can be incorporated into the type of models used here (Thingstad et al. 1996), but Havskum and Hansen (1997) did not detect bacterivory by pigmented protists in this experiment.

The general pattern of change observed in the ciliate population in the experimental system was in accordance with the predicted behavior of the idealized ciliate population of the model. In the model, ciliates represented organisms preying on heterotrophic flagellates and phytoplankton. Because this predation reduces both competition and predation on the bacteria, the predicted effect of ciliates on bacterial production is large (proportional to C^2). In the experimental system with its subpopulations of filamentous bacteria and large chain-forming diatoms, this simple representation may miss important trophic interactions. Phytoplankton too large to serve as prey for ciliates and bacteria too large to serve as prey for heterotrophic flagellates would remain as competitors for bacteria $< 2 \mu\text{m}$, even when the ciliate population increases. A proper representation of the predatory loss of the large phytoplankters would require inclusion in the model of heterotrophic dinoflagellates and mesozooplankton able to feed on prey larger than that captured by ciliates. We have not tried to extend the model description by assuming, e.g., direct predation on a subpopulation of filamentous bacteria by ciliates, but qualitatively this predation would be expected to diminish the large difference predicted by our model

for the effects of ciliate predation on bacterial biomass (proportional to C) and bacterial production (proportional to C^2) because an increase in ciliate biomass then no longer represents the same reduction in predation pressure on the bacterial community. In the enclosure receiving phosphate, the ciliate biomass increased by a factor of 18 through the experimental period (Fig. 8). According to the simple model, the bacterial production should then have increased by a factor of around $18^2 = 324$. Our thymidine-based estimates of bacterial production in enclosures receiving phosphate increased by a factor of only 12–14, and a scatter diagram of bacterial production versus ciliate biomass (Fig. 11) suggests a linear rather than a second order relationship. This is the relationship that would be expected if competition is not affected by ciliate predation. We therefore suspect that inclusion of the effects of filamentous bacteria and large phytoplankton would improve the fit between model and experiment.

In the experimental data, there is an approximate doubling in bacterial production observed between the first and second day of the experiment, a pattern not reproducible with our hybrid model. Such a discrepancy could be a possible result of our steady state assumption. Using the differential equations equivalent to the steady state equations in Table 4, we have solved the full dynamic version of the model using the STELLA[®] program (4th order Runge Kutta algorithm, 0.025 h time step). As expected, removal of the steady state assumption introduces a jump in bacterial production in the

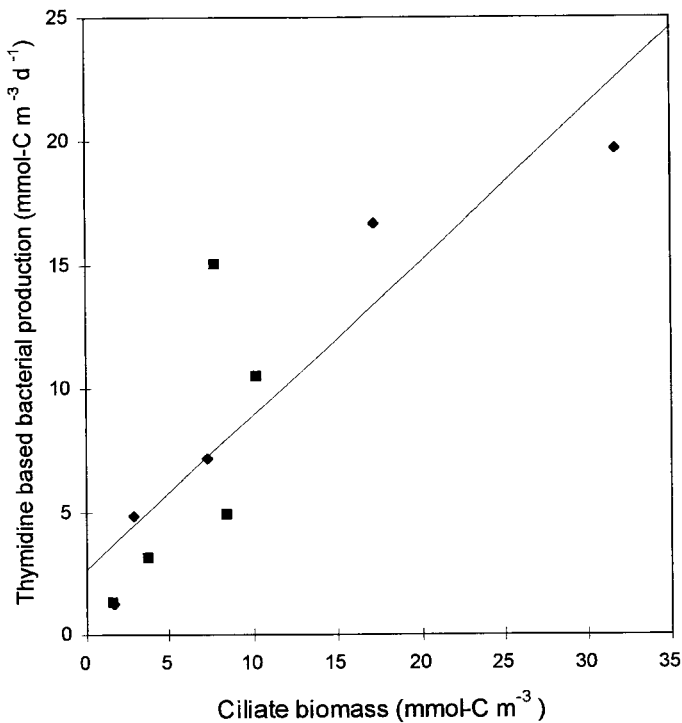


Fig. 11. Bacterial production versus ciliate biomass for the two enclosures K1 (squares) and P3 (diamonds) where ciliate biomass was determined. Regression line ($y = 2.7 + 0.63x$) is for all points.

initial phase (Fig. 12) and therefore gives a better reproduction of the observed pattern.

The hybrid model also gives a more rapid decline in phytoplankton and a larger increase in bacterial production than observed towards the end of the experiment. Again this may be a result of our steady state approximation. The full dynamic representation of the model has a more delayed peak in phytoplankton and a lower final bacterial production (Fig. 12) than the hybrid version. These effects would also be expected if higher predators or other mechanisms removing ciliates had been introduced.

A feature not explainable within the framework of our model is the observed sequence of primary production culminating before chlorophyll in enclosures receiving phosphate. This feature appears to be caused by a large diatom component dominated by *Chaetocheros wighamii* and small centric diatoms (Havskum and Hansen 1997) becoming silicate limited; silicate was depleted around 9 July in the enclosures receiving phosphate. For this subpopulation, growth rate limitation by silicate thus seemed to occur before the decrease in biomass. Our model assumes P limitation of phytoplankton growth rate and is not appropriate for Si-limited situations. A possible additional effect on phytoplankton growth rate may have been caused by the intermediary depletion of nitrate. Nitrate and phosphate were, however, supplied at a ratio above Redfield (20:1), and extremely short turnover times for orthophosphate combined with high alkaline phosphatase activity (data not shown) suggest that N limitation, if effective, must at least have occurred in parallel with a severe P limitation. Also in enclosures without added

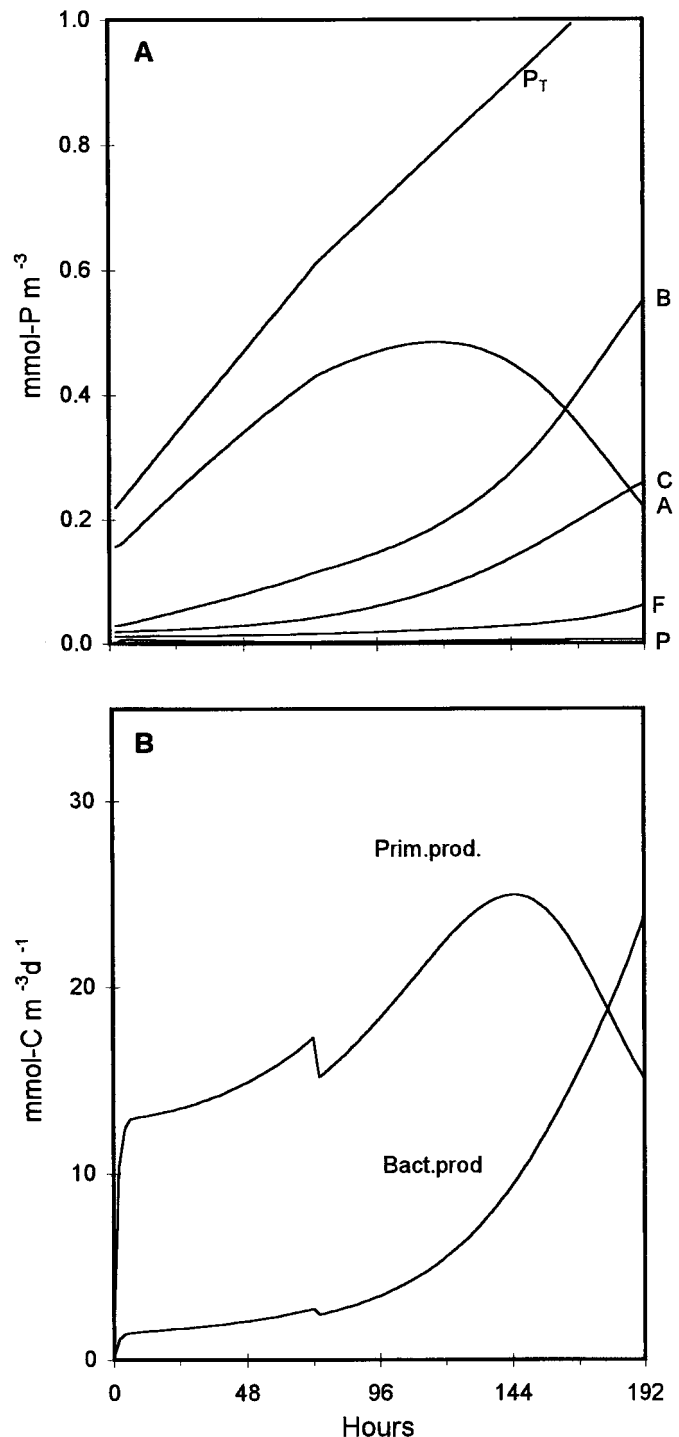


Fig. 12. Full dynamic solution of the model using the differential equation equivalents to the differential equations in Table 4. Biomasses (A) and bacterial and primary production (B) are shown for enclosures receiving phosphate. Carbon fluxes were calculated from the models' P fluxes by assuming a molar C:P ratio of 106 in phytoplankton and 50 in bacteria.

phosphate, we observed a continuous consumption of part of the added nitrate. High consumption of nitrate relative to phosphate has been described in axenic algal cultures and has been suggested (Collos 1992) to be caused by algal conversion of nitrate to dissolved organic N. Depletion of nitrate would in such a case not necessarily be a sign of N-limited growth rate.

One of the advantages of the analytical form of the steady state solution is that it allows a full analytical sensitivity analysis. As an example, the relative change $\Delta B/B$ in steady state bacterial biomass as the result of a relative change $\Delta\alpha_A/\alpha_A$ in phytoplankton affinity is given by the expression

$$\frac{\Delta B}{B} = \left(\frac{\alpha_A}{B} \frac{\partial B}{\partial \alpha_A} \right) \frac{\Delta \alpha_A}{\alpha_A}.$$

The sensitivity coefficient

$$\frac{\alpha_A}{B} \frac{\partial B}{\partial \alpha_A}$$

is thus a dimensionless proportionality factor between the two relative changes. A sensitivity coefficient of 2 thus means that a 1% change in the parameter gives a 2% change in the variable (at steady state). This finding can be used to summarize some interesting and not intuitively obvious properties of the model (Table 6). None of the sensitivity coefficients for bacterial biomass (B) or for the bacterial substrate (P) depend upon parameter values, or on total amount of available nutrient (P_t), or ciliate biomass (C). They are all fixed numbers (-1 , 0 , or 1), given by the structure of the model. Our data did not include any estimate of bacterial loss due to viral lysis, and the δ_B parameter in the model has been set to 0. With $\delta_B = 0$, the sensitivity coefficients for biomass F of heterotrophic flagellates also become fixed numbers (-1 , 0 , or 1). However, the somewhat counterintuitive effect is that inclusion of a bacterial loss rate due to viral lysis ($\delta_B \neq 0$) has no effect on bacterial biomass or production (sensitivity coefficients identical to 0), but it shifts the balance between phytoplankton and heterotrophic flagellate biomass towards phytoplankton:

$$\frac{\delta_B}{A} \frac{\partial A}{\partial \delta_B} > 0$$

$$\frac{\delta_B}{F} \frac{\partial F}{\partial \delta_B} < 0.$$

Increasing the α values also has some counterintuitive effects; a change to larger α_B will not affect the bacteria at steady state but will shift the biomass balance from phytoplankton to heterotrophic flagellates. An increase in α_A , however, will increase phytoplankton biomass while reducing both phosphate and heterotrophic flagellates. Increasing α_F will increase phytoplankton biomass at the expense of both flagellates and bacteria.

Our simple model for P-limited bacterial growth was able to reproduce the difference between enclosures receiving glycine and phosphate and the broad pattern of succession consisting of an autotrophic phase followed by a heterotrophic phase in all enclosures. The culmination of phytoplankton in the middle of the experimental period, the rapid in-

Table 6. Sensitivity coefficients of the variables with respect to the parameters (see Table 4).

	α_B	α_A	α_F	α_C	Y_F	δ_B	C	P_t
General								
P	0	-1	0	1	0	0	1	0
B	0	0	-1	1	-1	0	1	0
A	$-\frac{\alpha_B \alpha_C C}{\alpha_F \alpha_A A}$	$\left(1 + \frac{\alpha_B}{\alpha_F}\right) \frac{\alpha_C C}{\alpha_A A}$	$\frac{1}{\alpha_F A} \left[\left(\frac{\alpha_B + 1}{\alpha_A}\right) \alpha_C C - \delta_B \right]$	$-\left(1 + \frac{\alpha_B}{Y_F \alpha_F} + \frac{\alpha_B}{\alpha_F}\right) \frac{\alpha_C C}{\alpha_A A}$	$\frac{\alpha_C C}{Y_F \alpha_F A}$	$\frac{\delta_B}{\alpha_F A}$	$-\left(1 + \frac{\alpha_A}{Y_F \alpha_F} + \frac{\alpha_B}{\alpha_F}\right) \frac{\alpha_C C}{\alpha_A A}$	$\frac{P_t}{A}$
F	$\frac{\alpha_B \alpha_C C}{\alpha_A \alpha_F F}$	$-\frac{\alpha_B \alpha_C C}{\alpha_A \alpha_F F}$	-1	$\frac{\alpha_B \alpha_C C}{\alpha_A \alpha_F F}$	0	$-\frac{\delta_B}{\alpha_F F}$	$\frac{\alpha_B \alpha_C C}{\alpha_A \alpha_F F}$	0
Actual values*								
P	0	-1	0	1	0	0	1	0
B	0	0	-1	1	-1	0	1	0
A	$\frac{3.13C}{2.1C - P_t}$	$\frac{-0.63C}{2.1C - 1P_t}$	$\frac{-2.1C}{2.1C - P_t}$	$\frac{2.1C}{2.1C - P_t}$	$\frac{-1.47C}{2.1C - P_t}$	0	$\frac{-2.09C}{2.1C - P_t}$	$\frac{-P_t}{2.1C - P_t}$
F	1	-1	-1	1	0	0	1	0

crease in bacterial production in the latter half of the experimental period, and the near-exponential growth in ciliates are also features reproduced by the model.

Although reasonably successful in reproducing major qualitative aspects of the experimental system, the hybrid differential equation–steady state approach used here has clear limitations for studies where high temporal resolution is desired. The intentionally low number of trophic levels and interactions also restricted our ability to account for interesting and probably dynamically important aspects caused by subpopulations with special characteristics. To overcome such difficulties, models with more trophic members, all fully described by differential equations (e.g., Baretta-Bekker et al. 1995, 1998), seem to be the only present option. The strength of the analytical approach used here is the possibility of deriving nontrivial and experimentally testable relationships such as shown in Eq. 9. Also, because numerical computation of algebraic equations is much faster than solving differential equations, this approach would also have practical potential if the microbial complex is to be incorporated in large 3-dimensional simulation models where computation time is crucial.

The most important aspect of this exercise is the theoretical and experimental demonstration of how a combination of predation and mineral nutrient limitation, rather than the availability of organic substrates, may control bacterial production and thus bacterial consumption of labile organic matter. The suggested minimalist model gave a first-order approximation to an explanation of the main mechanisms behind the pattern of succession following phosphate addition and the lack of response to glycine addition in our experimental system. A better fit to the observed data is probably obtainable by introducing more elaborate trophic interactions and by replacing the hybrid with a full differential equation description. However, this step should only be taken after the validity of the basic mechanism suggested here has been satisfactorily demonstrated and the implications properly understood.

References

- BARETTA-BEKKER, J. G., J. W. BARETTA, A. S. HANSEN, AND B. RIEMANN. 1998. An improved model of carbon and nutrient dynamics in the microbial food web in marine enclosures. *Mar. Ecol. Prog. Ser.* **14**: 91–108.
- , ———, AND E. KOCH RASMUSSEN. 1995. The microbial food web in the European regional seas ecosystem model. *Neth. J. Sea Res.* **33**: 363–379.
- BILLEN, G. 1990. Delayed development of bacterioplankton with respect to phytoplankton: A clue to understanding their trophic relationships. *Ergeb. Limnol.* **34**: 191–201.
- . 1991. Protein degradation aquatic environments, p. 123–143. *In* R. J. Chróst [ed.], *Microbial enzymes in aquatic environments*. Springer Verlag.
- BRATBAK, G., AND T. F. THINGSTAD. 1985. Phytoplankton–bacteria interactions: An apparent paradox? Analysis of a model system with both competition and commensalism. *Mar. Ecol. Prog. Ser.* **25**: 23–30.
- CARLSON, C. A., H. W. DUCKLOW, AND A. F. MICHAELS. 1994. Annual flux of dissolved organic carbon from the euphotic zone in the northwestern Sargasso Sea. *Nature* **371**: 405–408.
- COLLOS, Y. 1992. Nitrogen budgets and dissolved organic matter cycling. *Mar. Ecol. Prog. Ser.* **90**: 201–206.
- COPIN-MONTÉGUT, G., AND B. AVRIL. 1993. Vertical distribution and temporal variation of dissolved organic carbon in the north-west Mediterranean Sea. *Deep-Sea Res.* **40**: 1963–1972.
- COTNER, J. B., J. W. AMMERMAN, E. R. PEELE, AND E. BENTZEN. 1997. Phosphorus-limited bacterioplankton growth in the Sargasso Sea. *Aquat. Microb. Ecol.* **13**: 141–149.
- DANERI, G., B. RIEMANN, AND P. J. L. WILLIAMS. 1994. In situ bacterial production and growth yield measured by thymidine, leucine and fractionated dark oxygen uptake. *J. Plankton Res.* **16**: 105–113.
- DODGE, J. D. 1985. Marine dinoflagellates of the British Isles. Her Majesty's Stationery Office.
- EDLER, L. 1979. Recommendations for marine biological studies in the Baltic Sea. The Baltic Marine Biologist Publication, No. **5**: 1–38.
- EGGE, J. K., AND B. R. HEIMDAL. 1994. Blooms of phytoplankton including *Emiliania huxleyi* (Haptophyta): Effects of nutrient supply in different N:P ratios. *Sarsia* **79**: 333–348.
- ELSER, J. J., L. B. STABLER., AND R. P. HASSETT. 1995. Nutrient limitation of bacterial growth and rates of bacterivory in lakes and oceans. *Aquat. Microb. Ecol.* **9**: 105–110.
- FENCHEL, T. 1982. Ecology of heterotrophic microflagellates. IV. Quantitative occurrence and importance as bacterial consumers. *Mar. Ecol. Prog. Ser.* **9**: 35–42.
- FUHRMAN, J. A., AND F. AZAM. 1980. Bacterioplankton secondary production estimates for coastal waters of British Columbia, Antarctica and California. *Appl. Environ. Microbiol.* **39**: 1085–1095.
- HAVSKUM, H., AND A. HANSEN. 1997. Importance of pigmented and colorless nano-sized protists as grazers on nanoplankton in a phosphate-depleted Norwegian fjord and in enclosures. *Aquat. Microb. Ecol.* **12**: 139–151.
- JESPERSEN, A. M., AND K. CHRISTOFFERSEN. 1987. Measurements of chlorophyll *a* from phytoplankton using ethanol as extraction solvent. *Arch. Hydrobiol.* **109**: 445–454.
- JUMARS, P. A., D. L. PENRY, J. A. BAROSS, M. J. PERRY, AND B. W. FROST. 1989. Closing the microbial loop: Dissolved carbon pathway to heterotrophic bacteria from incomplete ingestion, digestion and absorption in animals. *Deep-Sea Res.* **36**: 483–495.
- KAHL, A. 1932. Urtiere oder protozoa. I. Wimpertiere oder Ciliata (Infusoria). 3. Spirotrichia. *In* F. Dahl [ed.], *Die Tierwelt Deutschlands und der angrenzenden Meeresteile*. Gustav Fishers Verlag, Jena.
- KEIL, R. G., AND D. L. KIRCHMAN. 1994. Abiotic transformation of labile protein to refractory protein in sea water. *Mar. Chem.* **45**: 187–196.
- KOROLEFF, F. 1976. Determination of phosphorus, p. 125–131. *In* K. Grasshoff [ed.], *Methods in seawater analysis*. Verlag Chemie.
- LEE, S., AND J. A. FUHRMAN. 1987. Relationships between biovolume and biomass of naturally derived marine bacterioplankton. *Appl. Environ. Microbiol.* **53**: 1298–1303.
- LEGENDRE, L., AND M. GOSSELIN. 1989. New production and export of organic matter to the deep ocean: Consequences of some recent discoveries. *Limnol. Oceanogr.* **34**: 1374–1380.
- LINDELL, M. J., W. GRANÉLI, AND L. J. TRANVIK. 1995. Enhanced bacterial growth in response to photochemical transformation of dissolved organic matter. *Limnol. Oceanogr.* **40**: 195–199.
- MONTAGNE, D. J. S., AND D. H. LYNN. 1991. Taxonomy of chloretotrichs, the major marine planktonic ciliates, with emphasis on the aloricate forms. *Mar. Microb. Food Webs* **5**: 59–74.
- MURRAY, J. W., R. T. BARBER, M. R. ROMAN, M. P. BACON, AND

- R. A. FEELY. 1994. Physical and biological controls on carbon cycling in the equatorial Pacific. *Science* **266**: 58–65.
- OLSEN, V., AND B. LUNDGREN. 1984. A compact eight-channel continuous flow analyzer for shipboard use. *Comm. Meet. Int. Counc. Explor. Sea C.M.-ICES/C* **19**.
- PARSONS, T. R., L. J. ALBRIGHT, F. WHITNEY, C. S. WONG, AND P. J. L. WILLIAMS. 1981. The effect of glucose on the productivity of seawater: An experimental approach using controlled aquatic ecosystems. *Mar. Environ. Res.* **4**: 229–242.
- PENGERUD, B., E. F. SKJOLDAL, AND T. F. THINGSTAD. 1987. The reciprocal interaction between degradation of glucose and ecosystem structure. Studies in mixed chemostat cultures of marine bacteria, algae, and bacterivorous nanoflagellates. *Mar. Ecol. Prog. Ser.* **35**: 111–117.
- PIRT, S. J. 1982. Maintenance energy: A general model for energy-limited and energy-sufficient growth. *Arch. Microbiol.* **133**: 300–302.
- POMEROY, L. R., J. E. SHELDON, W. M. SHELDON, JR., AND F. PETERS. 1995. Limits to growth and respiration of bacterioplankton in the Gulf of Mexico. *Mar. Ecol. Prog. Ser.* **117**: 259–268.
- PORTER, K. G., AND Y. S. FEIG. 1980. The use of DAPI for identifying and counting aquatic microflora. *Limnol. Oceanogr.* **25**: 943–948.
- RIEMANN, B., AND F. AZAM. 1992. Measurements of bacterial protein synthesis in eutrophic environments by means of leucine incorporation. *Mar. Microb. Food Webs* **6**: 91–105.
- , P. K. BJØRNSSEN, S. NEWELL, AND R. FALLON. 1987. Calculation of cell production of coastal marine bacteria based on measured incorporation of ³H-thymidine. *Limnol. Oceanogr.* **32**: 471–476.
- SIMON, M., AND F. AZAM. 1989. Protein content and protein synthesis rates of planktonic marine bacteria. *Mar. Ecol. Prog. Ser.* **51**: 201–213.
- SUTTLE, C. A., J. A. FUHRMAN, AND D. G. CAPONE. 1990. Rapid ammonium cycling and concentration-dependent partitioning of ammonium and phosphate: Implications for carbon transfer in planktonic communities. *Limnol. Oceanogr.* **35**: 424–433.
- THINGSTAD, T. F. 1987. Utilization of N, P, and organic C by heterotrophic bacteria. I. Outline of a chemostat theory with a consistent concept of maintenance metabolism. *Mar. Ecol. Prog. Ser.* **35**: 99–109.
- , Å. HAGSTRÖM, AND F. RASSOULZADEGAN. 1997. Accumulation of degradable DOC in surface waters: Is it caused by a malfunctioning microbial loop? *Limnol. Oceanogr.* **42**: 398–404.
- , H. HAVSKUM, K. GARDE, AND B. RIEMANN. 1996. On the strategy of “eating your competitor.” A mathematical analysis of algal mixotrophy. *Ecology* **77**: 2108–2118.
- , AND R. LIGNELL. 1997. Theoretical models for the control of bacterial growth rate, abundance, diversity and carbon demand. *Aquat. Microb. Ecol.* **13**: 19–27.
- , AND F. RASSOULZADEGAN. 1995. Nutrient limitations, microbial food webs, and “biological C-pumps”: Suggested interactions in P-limited Mediterranean. *Mar. Ecol. Prog. Ser.* **117**: 299–306.
- , E. F. SKJOLDAL, AND R. A. BOHNE. 1993. Phosphorus cycling and algal-bacterial competition in Sandsfjord, western Norway. *Mar. Ecol. Prog. Ser.* **99**: 239–259.
- , U. L. ZWEIFEL, AND F. RASSOULZADEGAN. 1998. P limitation of heterotrophic bacteria and phytoplankton in the north-west Mediterranean. *Limnol. Oceanogr.* **43**: 88–94.
- VAN LOOIJ, A., AND B. RIEMANN. 1993. Measurements of bacterial production in coastal marine environments: Application of a kinetic approach to correct for isotope dilution. *Mar. Ecol. Prog. Ser.* **102**: 97–104.
- WHEELER, P. A., AND D. L. KIRCHMAN. 1986. Utilization of inorganic and organic nitrogen by bacteria in marine systems. *Limnol. Oceanogr.* **31**: 998–1009.
- WILLIAMS, P. J. L. 1990. The importance of losses during microbial growth: Commentary on the physiology, measurement, and ecology of the release of dissolved organic material. *Mar. Microb. Food Webs* **4**: 175–206.
- . 1995. Evidence of the seasonal accumulation of carbon-rich dissolved organic material, its scale in comparison with changes in particulate material and the consequential effect on net C/N assimilation ratios. *Mar. Chem.* **51**: 17–29.
- , AND N. W. JENKINSON. 1982. A transportable micro-processor-controlled precise Winkler titration suitable for field station and shipboard use. *Limnol. Oceanogr.* **27**: 576–584.
- WINTERMANS, J. F. G. M., AND A. DE MOTTS. 1965. Spectrophotometric characteristics of chlorophylls *a* and *b* and their pheophytins in ethanol. *Biochim. Biophys. Acta* **109**: 448–453.
- YULL RHEE, G. 1972. Competition between a alga and an aquatic bacterium for phosphate. *Limnol. Oceanogr.* **17**: 505–514.
- ZWEIFEL, U. L., B. NORRMAN, AND Å. HAGSTRÖM. 1993. Consumption of dissolved organic carbon by bacteria and demand for inorganic nutrients. *Mar. Ecol. Prog. Ser.* **101**: 23–32.
- , J. WIKNER, AND Å. HAGSTRÖM. 1995. Dynamics of dissolved organic carbon in a coastal ecosystem. *Limnol. Oceanogr.* **40**: 299–305.

Received: 19 August 1997

Accepted: 10 July 1998

Amended: 14 August 1998